# An Inverse Method to Measure the Axial Modulus of Composite Materials Under Tension
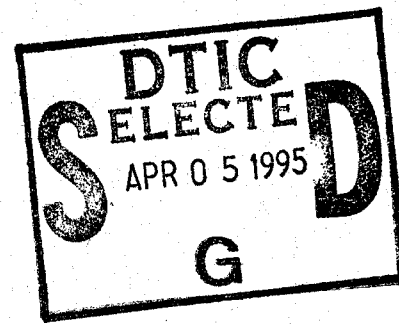
Andrew J. Hull
Submarine Sonar Department

DTIC
S ELECTE D
APR 0 5 1995
G

# Naval Undersea Warfare Center Division
## Newport, Rhode Island

19950404 157

# PREFACE

The investigation described in this report was sponsored by the Office of Naval Research in Washington, DC.

The technical reviewer for this report was S. A. Austin (Code 2141).

The author wishes to thank K. A. Holt for her help with the editing of the manuscript.

Reviewed and Approved:  3 January 1995

R. J. Martin
Acting Head, Submarine Sonar Department

# REPORT DOCUMENTATION PAGE

Public reporting burden for this collection of information is estimated to average 1 hour per response, including the time for reviewing instructions, searching existing data sources, gathering and maintaining the data needed, and completing and reviewing the collection of information. Send comments regarding this burden estimate or any other aspect of this collection of information, including suggestions for reducing this burden, to Washington Headquarters Services, Directorate for information Operations and Reports, 1215 Jefferson Davis Highway, Suite 1204, Arlington, VA 22202-4302, and to the Office of Management and Budget, Paperwork Reduction Project (0704-0188), Washington, DC 20503.

| 1. AGENCY USE ONLY (Leave Blank) | 2. REPORT DATE 3 January 1995 | 3. REPORT TYPE AND DATES COVERED Final |
|---|---|---|

**4. TITLE AND SUBTITLE**

**An Inverse Method to Measure the Axial Modulus of Composite Materials Under Tension**

**5. FUNDING NUMBERS**

**6. AUTHOR(S)**

Andrew J. Hull

**7. PERFORMING ORGANIZATION NAME(S) AND ADDRESS(ES)**

Naval Undersea Warfare Center
Detachment New London
New London, Connecticut 06320

Accesion For

| NTIS CRA&I | ☒ |
| DTIC TAB | ☐ |
| Unannounced | ☐ |
| Justification | |

By

Distribution /

Availability Codes

| Dist | Avail and / or Special |
| A-1 | |

**8. PERFORMING ORGANIZATION REPORT NUMBER**

TR 10,801

**9. SPONSORING/MONITORING AGENCY NAME(S) AND ADDRESS(ES)**

Office of Naval Research
800 North Quincy Street
Arlington, VA 22217-5000

**10. SPONSORING/MONITORING AGENCY REPORT NUMBER**

**11. SUPPLEMENTARY NOTES**

**12a. DISTRIBUTION/AVAILABILITY STATEMENT**

Approved for public release; distribution is unlimited.

**12b. DISTRIBUTION CODE**

**13. ABSTRACT (Maximum 200 words)**

In this report, an inverse method is developed to measure the axial modulus of materials subjected to tensile loads. The approach is intended for use on long composite structures whose modulus is frequency dependent. The governing differential equations of a laboratory test configuration are solved and then inverted at three locations that correspond to sensor transfer functions. These three equations are next combined in such a way that the complex-valued axial modulus is equal to a function of the measured data and the known system parameters. This expression is a closed-form measurement of the modulus at each test frequency. An experiment is included to validate the method. Comparisons between the transfer function data and the model expressed with the measured modulus are in close agreement.

DTIC QUALITY INSPECTED 3

**14. SUBJECT TERMS**
Axial Modulus, Composite Materials, Inverse Method, Long Composite Structure, Loss, Sensor Transfer Function, Stiffness, Tensile Loads, Tensioned Bar

**15. NUMBER OF PAGES**
22

**16. PRICE CODE**

| 17. SECURITY CLASSIFICATION OF REPORT | 18. SECURITY CLASSIFICATION OF THIS PAGE | 19. SECURITY CLASSIFICATION OF ABSTRACT | 20. LIMITATION OF ABSTRACT |
|---|---|---|---|
| UNCLASSIFIED | UNCLASSIFIED | UNCLASSIFIED | SAR |

# TABLE OF CONTENTS

# LIST OF ILLUSTRATIONS

# AN INVERSE METHOD TO MEASURE THE AXIAL MODULUS OF COMPOSITE MATERIALS UNDER TENSION

## 1. INTRODUCTION

Measuring the stiffness and loss properties of materials is extremely important because such properties significantly contribute to the dynamic response of a structure. Resonant techniques to measure stiffness and loss have been used by researchers for many years [1-4]. This approach is based on measuring the eigenvalues of a structure and comparing them to eigenvalues of a model of the same structure. During the comparison, stiffness and loss properties are identified. However, the structure must have well-defined eigenvalues and eigenvectors for the method to be successful. Bars that are placed under tension with masses or ropes do not have closed-form eigenvectors, and their eigenvalues must be calculated with a transcendental equation. Additionally, this test only allows measurements at resonances. Material testing machines [5-7], which are designed to excite pieces of materials in a manner that allows investigation of stiffness and loss, provide yet another measurement tool. However, the typically small test samples cannot be subjected to significant tensile forces because of their size. Comparison of analytical models to measured frequency response functions is another approach for measuring stiffness and loss parameters [8-14]. It is unfortunate that most of these methods tend to be computationally intensive, and the fitting routines do not always converge to the correct answer, especially when more than one unknown parameter of the model must be estimated.

In this report, an inverse method is derived to measure the axial modulus of bars under tension. This method is intended for use primarily on long composite structures whose axial modulus is tension (and frequency) dependent. Such tension dependency is usually a result of the load share shifting from one material to another or a change in material rigidity when the structure is subjected to a tensile force. The governing differential equations of a bar with displacement input at one end and terminated to ground with a mass, spring, and damper at the other end are solved to yield a model of the displacement and force in the bar. The force and

displacement equations are then written to correspond to three sensor transfer functions. These three equations and the corresponding data are next combined to yield a closed-form value of the axial modulus (including a loss term) at each frequency where a measurement was made. The model is then computed with the measured moduli and is compared to the data.

Use of this model with the inverse method corresponds to the physical testing configuration in the Axial Vibration Test Facility (AVTF) at the Naval Undersea Warfare Center (NUWC), Detachment New London, as shown in figure 1. The AVTF has been designed to provide a simple procedure for testing bars under varying tensions and temperatures. The longitudinal shaker at the forward end of the bar provides axial excitation to the structure. A rope attached to the aft end of the bar and to a tension drum allows the tension to be adjusted. A mass is attached between the bar and the rope to ensure that the impedance change at the end of the bar is sufficiently large to allow accurate modeling of the rope behavior by a spring and damper rather than by a continuous media expression. The entire unit is surrounded by an air-conditioned PVC duct to permit temperature-dependent testing. Impedance heads are attached to the forward and aft ends of the bar to collect data during a test. Each impedance head consists of a single force transducer and accelerometer. A load cell that measures the tension on the structure is located between the rope and the mass. Although the test and inverse method were designed primarily for materials with "tension only" behavior, there is no requirement that the material undergoing the test exhibit this characteristic.
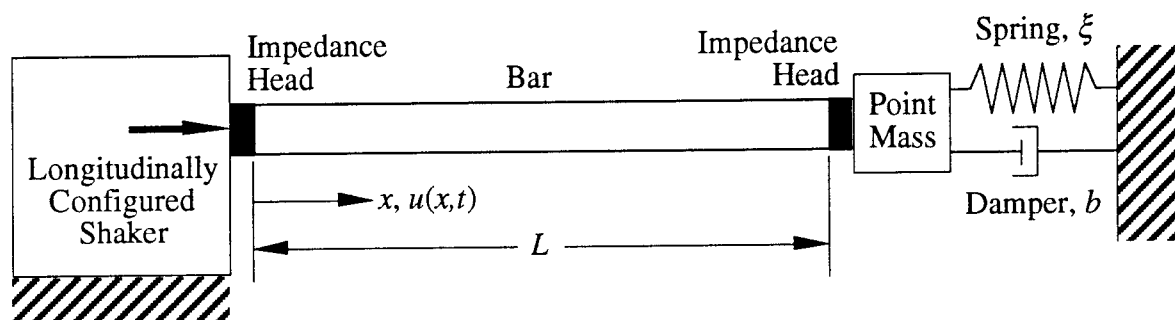


Figure 1. Laboratory Configuration

## 2. SYSTEM MODEL

The system model is a longitudinal bar with a displacement-driven boundary condition at one end and a mechanically grounded spring and damper at the other. There is a point mass attached between the bar and the spring and damper. The governing partial differential equation on the domain of the bar is the wave equation and is expressed as

$$\frac{\partial^2 u(x,t)}{\partial t^2} - c^2 \frac{\partial^2 u(x,t)}{\partial x^2} = 0 \ , \tag{1}$$

where $u(x,t)$ is the axial displacement (m), $x$ is the spatial location (m), $t$ is time (s), and $c$ is the wave speed (m/s). The wave speed is equal to

$$c = \sqrt{\frac{E}{\rho}} \ , \tag{2}$$

where $E$ is the axial modulus (N/m$^2$) and $\rho$ is the density of the bar (kg/m$^3$). The energy attenuation in the bar is defined with a structural damping law and therefore the modulus is a complex number. Note that a structural loss law requires that any solution obtained be in the frequency domain represented by

$$u(x,t) = U(x)e^{i\omega t} \ , \tag{3}$$

where $U(x)$ is a spatial displacement function (m), $i$ is the square root of -1, and $\omega$ is frequency (rad/s). Additionally, the wave speed in the bar becomes a complex number. The real part of the wave speed corresponds to energy transmission and the imaginary part corresponds to energy attenuation.

The longitudinal shaker is modeled as a harmonic boundary condition in the axial direction at $x = 0$ as

$$u(0,t) = U_0 e^{i\omega t} \ , \tag{4}$$

where $U_0$ is the amplitude of the displacement at the boundary (m). The mass and termination rope are modeled as a boundary condition at $x = L$ by a point mass attached to a parallel spring and viscous damper connected at one end to the bar and at the other end to mechanical ground

3

(zero displacement). This equation is derived as follows by equating the longitudinal force at the end of the bar to the forces in the mass, damper, and spring:

$$AE\frac{\partial u(L,t)}{\partial x} = -m\frac{\partial^2 u(L,t)}{\partial t^2} - b\frac{\partial u(L,t)}{\partial t} - \xi u(L,t) \ , \tag{5}$$

where $A$ is the cross-sectional area of the bar ($m^2$), $m$ is the point mass (kg), $b$ is the viscous loss coefficient of the damper (Ns/m), and $\xi$ is the spring constant (N/m).

The steady-state displacement $U(x)$, normalized by the input displacement $U_0$, is [15]

$$\frac{U(x)}{U_0} = \frac{\left[AEik - \xi + m\omega^2 - bi\omega\right]e^{-ik(L-x)} + \left[AEik + \xi - m\omega^2 + bi\omega\right]e^{ik(L-x)}}{\left[AEik + \xi - m\omega^2 + bi\omega\right]e^{ikL} + \left[AEik - \xi + m\omega^2 - bi\omega\right]e^{-ikL}} \tag{6}$$

and the steady-state force $F(x)$, normalized by the input displacement $U_0$, is

$$\frac{F(x)}{U_0} = \frac{AEik\left\{\left[AEik - \xi + m\omega^2 - bi\omega\right]e^{-ik(L-x)} - \left[AEik + \xi - m\omega^2 + bi\omega\right]e^{ik(L-x)}\right\}}{\left[AEik + \xi - m\omega^2 + bi\omega\right]e^{ikL} + \left[AEik - \xi + m\omega^2 - bi\omega\right]e^{-ikL}} \ , \tag{7}$$

where $k$ is the complex-valued extensional wavenumber of the structure (rad/m) defined by

$$k = \frac{\omega}{c} \ . \tag{8}$$

The known parameters in equations (6) and (7) are the point mass $m$, the density of the bar $\rho$, the cross-sectional area of the bar $A$, and the length $L$. The inversion of equations (6) and (7) at the sensor locations will allow for a measurement of the unknown axial modulus $E$, spring constant $\xi$, and viscous loss coefficient $b$. This technique is described next.

## 3. INVERSION OF THE SYSTEM MODEL

The experiment has four sensors to collect data that are in the form of transfer functions between pairs of sensors; thus three independent measurements are possible. The three transfer function measurements are the forward displacement divided by the aft displacement, the forward force divided by the aft displacement, and the forward displacement divided by the aft force. Their theoretical form can be rewritten using equations (6) and (7) and the

relationships between the exponential and trigonometric functions. These transfer functions are the theoretical form of the measured frequency domain data. Denoted $T_1$, $T_2$, and $T_3$, they are expressed as

$$\frac{U_0}{U(L)} = \cos(kL) + \frac{(\xi - m\omega^2 + bi\omega)}{AEk}\sin(kL) = T_1 \ , \tag{9}$$

$$\frac{F(0)}{U(L)} = AEk\sin(kL) - (\xi - m\omega^2 + bi\omega)\cos(kL) = T_2 \ , \tag{10}$$

and

$$\frac{U_0}{F(L)} = \frac{-\cos(kL)}{(\xi - m\omega^2 + bi\omega)} - \frac{\sin(kL)}{AEk} = T_3 \ . \tag{11}$$

The mass-damper-spring term can be solved for by dividing equation (9) by equation (11) which yields

$$\xi - m\omega^2 + bi\omega = \frac{-T_1}{T_3} \ . \tag{12}$$

Because of their relative size, the magnitudes of $T_2$ and $T_3$ are now changed based on equation (12). For most experiments, $T_1$ is of order 1, $T_2$ is of order $10^5$, and $T_3$ is of order $10^{-5}$. To reduce numerical errors, it is desirable to have all the data values of the same relative magnitude, which is accomplished by dividing equation (10) by equation (12), multiplying equation (11) by equation (12), and leaving equation (9) unchanged, resulting in

$$\cos(kL) + \frac{(\xi - m\omega^2 + bi\omega)}{AEk}\sin(kL) = T_1 = R_1 \ , \tag{13}$$

$$\frac{AEk}{(\xi - m\omega^2 + bi\omega)}\sin(kL) - \cos(kL) = \frac{-T_2 T_3}{T_1} = R_2 \ , \tag{14}$$

and

$$-\cos(kL) - \frac{(\xi - m\omega^2 + bi\omega)}{AEk}\sin(kL) = -T_1 = R_3 \ . \tag{15}$$

Equation (13) is now rewritten as

$$AEk = \frac{(\xi - m\omega^2 + bi\omega)\sin(kL)}{R_1 - \cos(kL)} \;, \tag{16}$$

and equation (14) is rewritten as

$$AEk = \frac{(\xi - m\omega^2 + bi\omega)[R_2 + \cos(kL)]}{\sin(kL)} \;. \tag{17}$$

Equating equations (16) and (17) and applying a Pythagorean relationship produces

$$\cos(kL) = \cos\{[\mathrm{Re}(k) + i\,\mathrm{Im}(k)]L\} = \frac{R_2 R_1 - 1}{R_2 - R_1} = \phi \;, \tag{18}$$

where $\phi$ is a complex number, Re denotes the real part of $k$, and Im denotes the imaginary part of $k$. Using an angle-sum relationship on the cosine term in equation (18) and separating the equation into real and imaginary parts yields

$$\cos[\mathrm{Re}(k)L]\cosh[\mathrm{Im}(k)L] = \mathrm{Re}(\phi) \tag{19}$$

and

$$\sin[\mathrm{Re}(k)L]\sinh[\mathrm{Im}(k)L] = -\mathrm{Im}(\phi) \;. \tag{20}$$

Equation (15) is now rewritten as

$$AEk = \frac{-(\xi - m\omega^2 + bi\omega)}{[R_3 + \cos(kL)]}\sin(kL) = \frac{-(\xi - m\omega^2 + bi\omega)}{(R_3 + \phi)}\sin(kL) \;. \tag{21}$$

The right-hand side of equation (21) is now set equal to the right-hand side of equation (17), which produces

$$\sin(kL) = \sin\{[\mathrm{Re}(k) + i\,\mathrm{Im}(k)]L\} = \pm\sqrt{(-1)(R_2 + \phi)(R_3 + \phi)} = \pm\psi \;, \tag{22}$$

where $\psi$ is a complex number and the sign of equation (22) is determined below. Using an angle-sum relationship on the sine term in equation (22) and separating the equation into real and imaginary parts yields

$$\sin[\mathrm{Re}(k)L]\cosh[\mathrm{Im}(k)L] = \mathrm{Re}(\psi) \tag{23}$$

and

$$\cos[\mathrm{Re}(k)L]\sinh[\mathrm{Im}(k)L] = \mathrm{Im}(\psi) \;. \tag{24}$$

Combining equations (19) and (23) yields

$$\text{Re}(k) = \frac{1}{L}\arctan\left[\frac{\text{Re}(\psi)}{\text{Re}(\phi)}\right] + \frac{n\pi}{L} ,$$

(25)

where $n$ is an integer greater than or equal to zero and is determined as shown below. Combining equation (20) and equation (23) yields

$$\text{Im}(k) = \frac{1}{L}\log_e\left\{\frac{\sin[\text{Re}(k)L]}{\text{Re}(\psi) + \text{Im}(\phi)}\right\} .$$

(26)

Now that the real and imaginary parts of the wavenumber $k$ are known, the complex-valued modulus of elasticity can be determined at each frequency with

$$E = \text{Re}(E) + i\,\text{Im}(E) = \frac{\rho\omega^2}{[\text{Re}(k) + i\,\text{Im}(k)]^2} .$$

(27)

The signs of $E$ are used to determine the sign of $\psi$ and the value of $n$. Note that $\text{Re}(E)$ and $\text{Im}(E)$ are strictly positive by definition. To ensure this condition, equation (27) will only be valid when $\text{Re}(k)$ is greater than zero and $\text{Im}(k)$ is less than zero. The minimum value of $\text{Re}(k)$ greater than zero requires that

$$0 < \frac{1}{L}\arctan\left[\frac{\text{Re}(\psi)}{\text{Re}(\phi)}\right] < \frac{\pi}{L} .$$

(28)

If the condition listed in equation (28) is violated, then $m\pi/L$ (where $m$ is an integer) must be added to the middle term of equation (28) to make the inequality hold. The integer $n$ is now set equal to zero. Next, $\text{Im}(k)$ less than zero requires that

$$0 < \frac{\sin[\text{Re}(k)L]}{\text{Re}(\psi) + \text{Im}(\phi)} < 1 .$$

(29)

For the right-hand side inequality to hold, it is necessary for

$$\left|\,\text{Re}(\psi) + \text{Im}(\phi)\,\right| > \left|\,\sin[\text{Re}(k)L]\,\right| .$$

(30)

If this inequality is not valid, then the sign of $\psi$ must be changed and $\text{Re}(k)$ in equation (25) must be recalculated. For the left-hand side inequality in equation (29) to hold requires that

$$\frac{\sin[\text{Re}(k)L]}{\text{Re}(\psi) + \text{Im}(\phi)} > 0 \ . \tag{31}$$

If this condition is violated, then $\pi/L$ must be added to $\text{Re}(k)$ to change the sign of the numerator in equation (31). Finally, either equation (9), (10), or (11) has to be solved with the estimated values of $E$ (and $k$) to determine if the theoretical transfer function matches the data. If it does not, the integer $n$ has to be increased by adding two, and the inequality checks in equations (29), (30), and (31) must be repeated.

## 4. EXPERIMENT

An experiment was conducted to validate the inverse method. A polyurethane bar with longitudinal polyester stiffeners was placed in tension as shown in figure 1. The bar had a density of 1100 kg/m$^3$, a cross-sectional area of 2.63 x 10$^{-4}$ m$^2$, and a length of 35.7 m. It was placed under 890 N of tension, with a point mass weight of 13.6 kg. The data from the force transducers and accelerometers were taken with an HP3562 dynamic signal analyzer. The analyzer converts the raw data from the time domain to the frequency domain. The test was run with a frequency range between 4 and 100 Hz. The data were collected with a logarithmic weight in frequency; however, for clarity, they are displayed with a linear frequency scale. The data that were collected with accelerometers must be changed to correspond to displacements because the transfer functions derived above were developed using displacement-based relationships. This is accomplished by dividing the accelerometer data by $-\omega^2$.

The first step was to determine the stiffness and viscous loss coefficient of the termination rope by applying equation (12) to the data. Analysis of equation (12) shows a single minimum of the transfer function. The data to the left of the transfer function minimum are stiffness dominated and were used to evaluate the stiffness of the rope. The following equation, derived from the real part of equation (12), was used:

$$\xi = \frac{1}{N} \sum_{j=1}^{N} \left[ m\omega_j^2 - \text{Re}\left( \frac{T_1(\omega_j)}{T_3(\omega_j)} \right) \right] , \tag{32}$$

where $N$ is the total number of data points to the left of the minimum and $j$ is a counter that corresponds to each frequency and data point at that frequency. This calculation produced a model stiffness of 33600 N. The viscous loss coefficient was determined using the imaginary part of equation (12) as

$$b = \frac{-1}{\omega_r} \text{Im}\left[ \frac{T_1(\omega_r)}{T_3(\omega_r)} \right] , \tag{33}$$

where $\omega_r$ corresponds to the resonance frequency of the spring-damper-mass system, which is also the transfer function minimum ($f_r = 9.55$ Hz). This calculation resulted in a viscous loss coefficient of 31.8 Ns/m. The data to the right of the transfer function minimum are not used to extract any system parameters because they are mass dominated. However, the estimated transfer function is compared to the measured transfer function at these points. Figure 2 is a plot of the data $[-T_1(\omega) / T_3(\omega)]$ and the model ($\xi - m\omega^2 + bi\omega$) fit to the data. Physically, this shows the (negative) aft force divided by the aft displacement. The solid line depicts the model and the X's depict the data. Note that, for this example, the model fits the data everywhere, even in the region where the system response is mass dominated. Additionally, the spring constant and viscous loss coefficient are well modeled by constant values in frequency.

Equations (13)-(31) were applied to the data, and the resulting axial modulus of the material was found. Figure 3 is a plot of the axial modulus versus frequency. The upper plot is the real part of $E$ and the lower plot is the loss factor ($\text{Im}(E)/\text{Re}(E)$). The data are shown with X's and an ordinary least square (OLS) straight-line fit is shown with the solid line. The data points at resonance that are yielding extremely large and small values of the modulus were not used in computing the OLS straight-line fit . Although a straight line was fit to the extracted modulus for this case, it is not necessary to use a linear estimate of the modulus. For

9

some materials it is likely that a polynomial fit to the modulus will produce more accurate results.

Figure 4 is a plot of the aft displacement divided by the forward displacement, which corresponds to the term $1/T_1$ from equation (9). Figure 5 is a plot of the forward force divided by the aft displacement, which corresponds to the term $T_2$ from equation (10). Figure 6 shows the aft force divided by the forward displacement, which corresponds to the term $1/T_3$ from equation (11). In figures 4, 5, and 6, the solid line is the model computed with a modulus value determined using the OLS method of figure 3. The model is depicted using a solid line and the data are shown using X's. For all three transfer functions, there is reasonable agreement between the data and model. As the frequency increases, there are slight variations between the model and the data. It is believed that these variations are caused by a phase mismatch between sensor pairs during the measurement process.
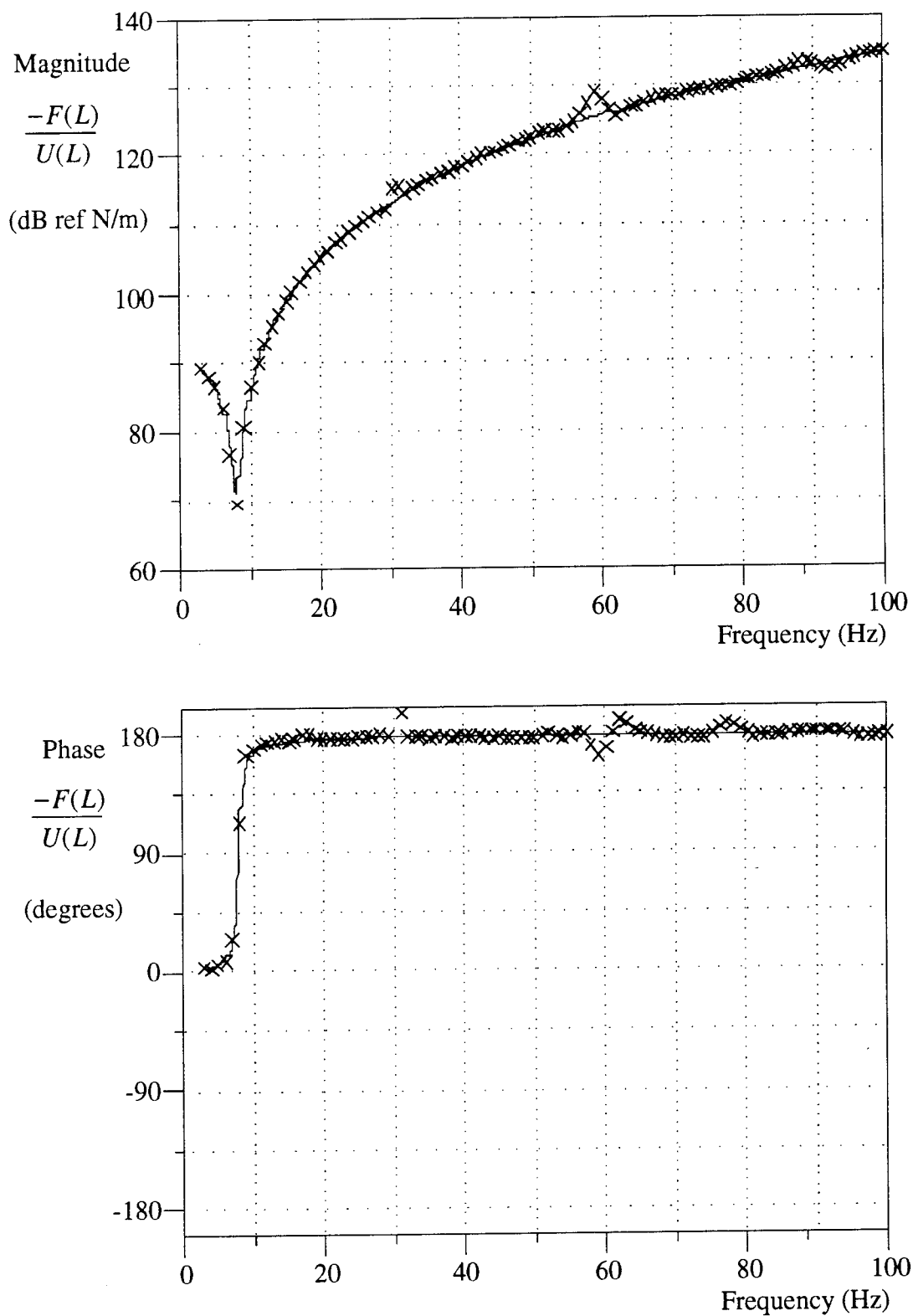
Figure 2. Transfer Function of Aft Force Divided by Aft Displacement With
Model Depicted as Solid Line and Experimental Data as X's
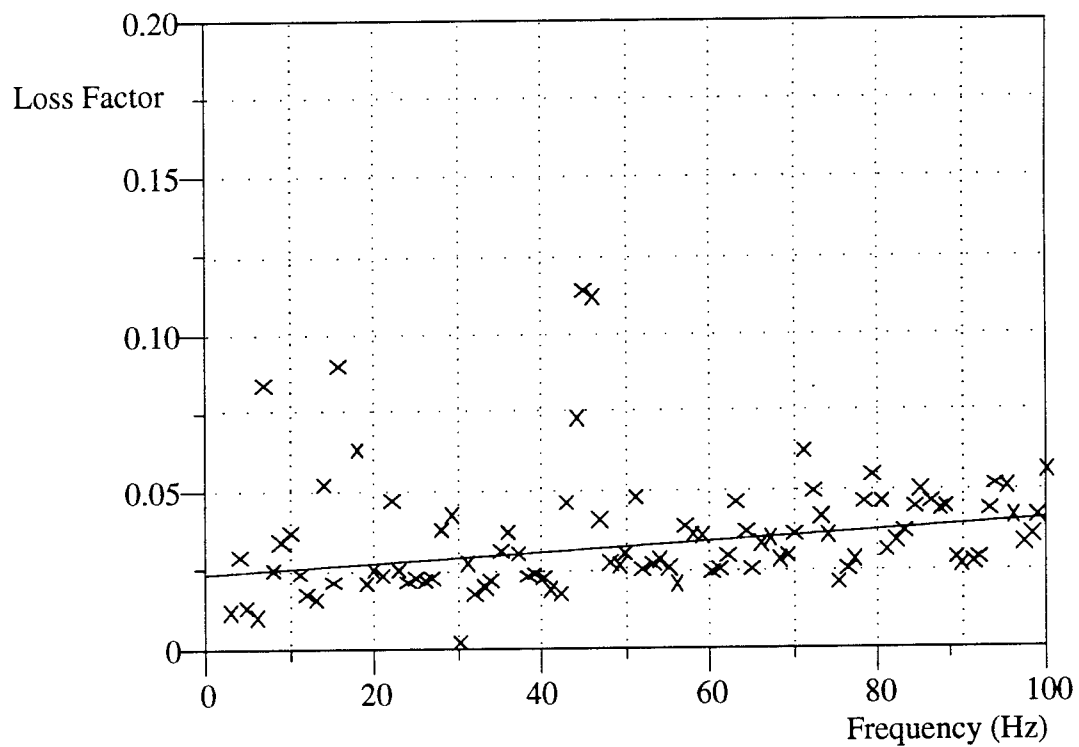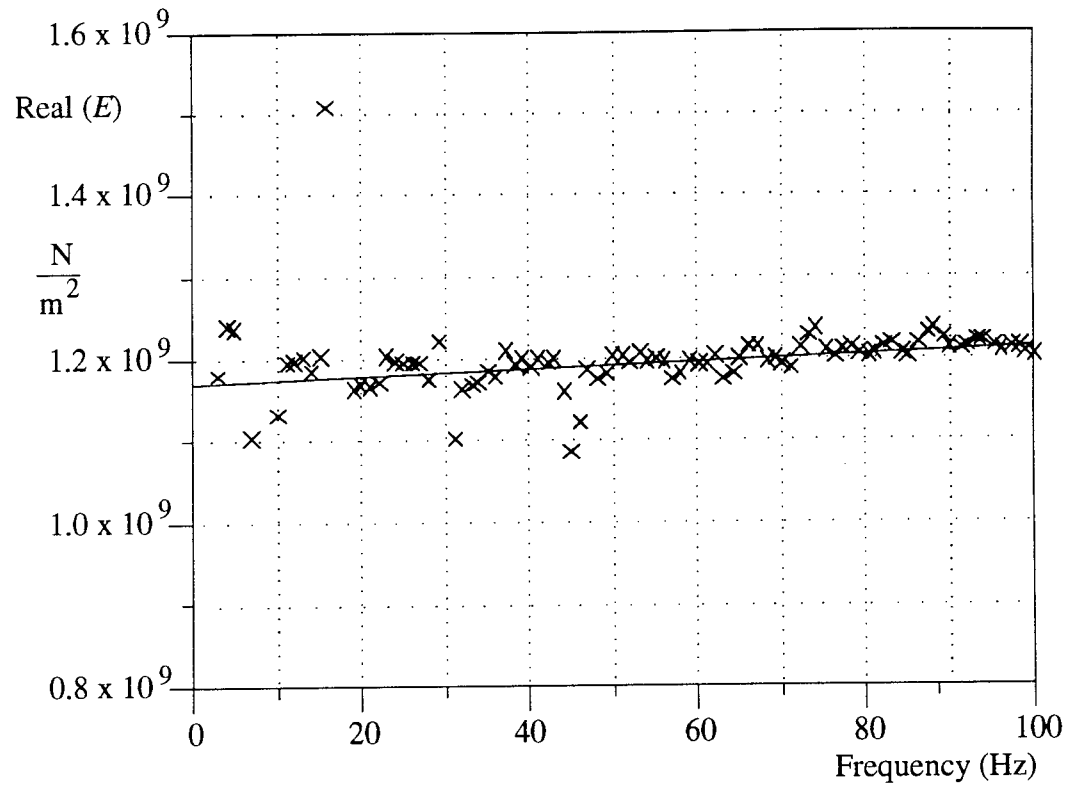
11

Figure 3. Real Part of Axial Modulus and Corresponding Loss Factor With OLS
Straight-Line Fit Depicted as Solid Line and Discrete Data as X's
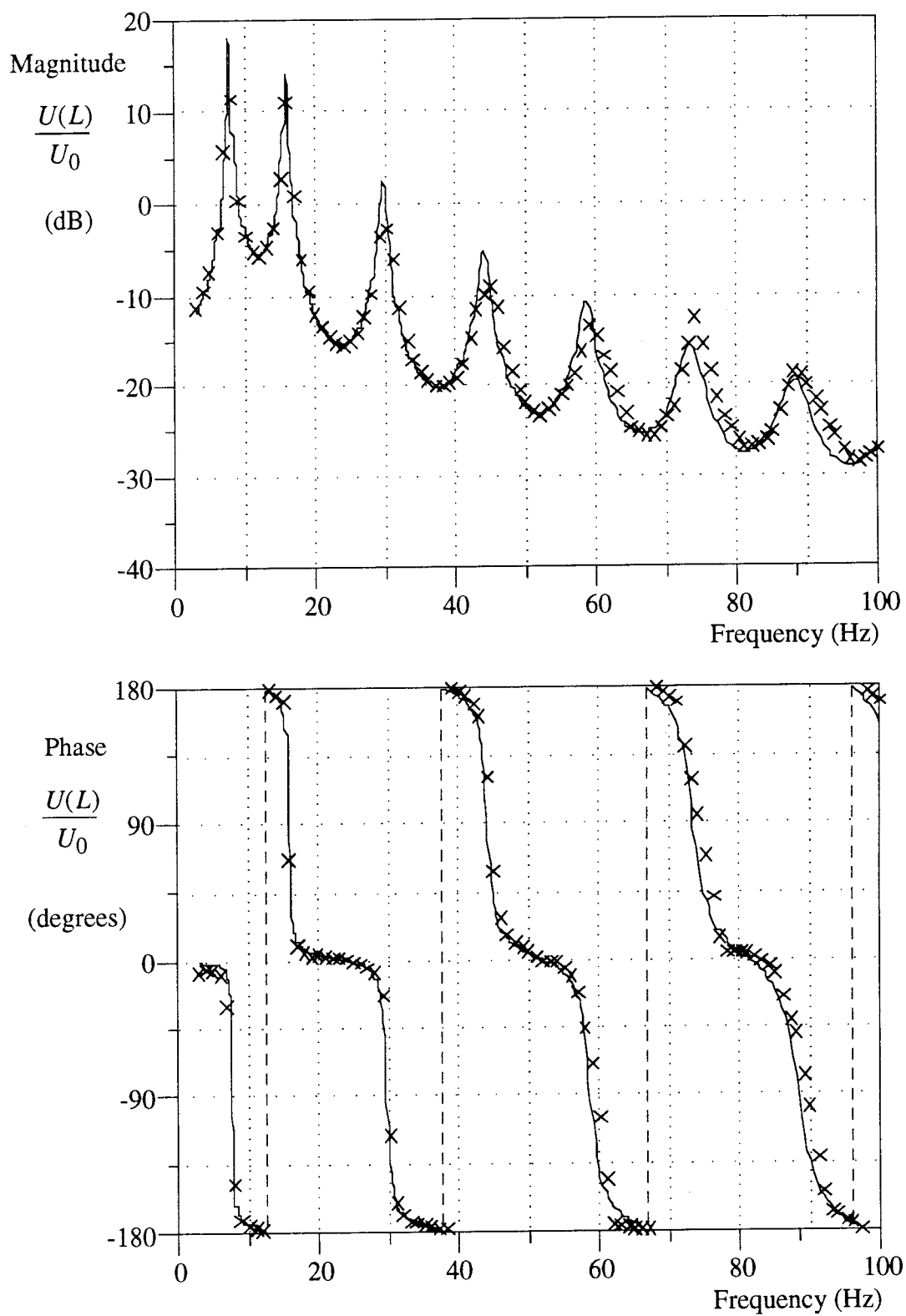
Figure 4.  Transfer Function of Aft Displacement Divided by Forward Displacement
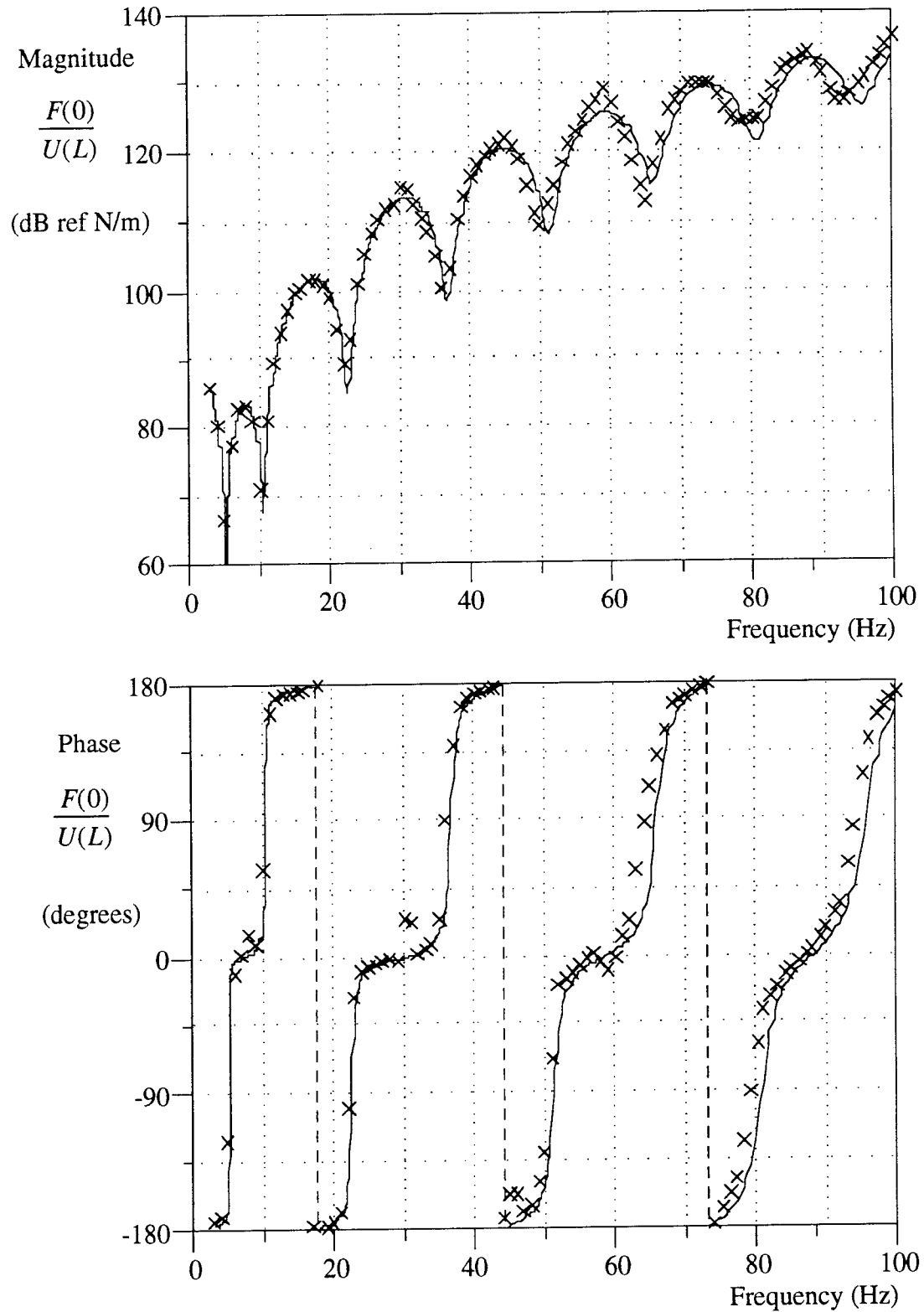With Model Depicted as Solid Line and Experimental Data as X's

Figure 5.  Transfer Function of Forward Force Divided by Aft Displacement
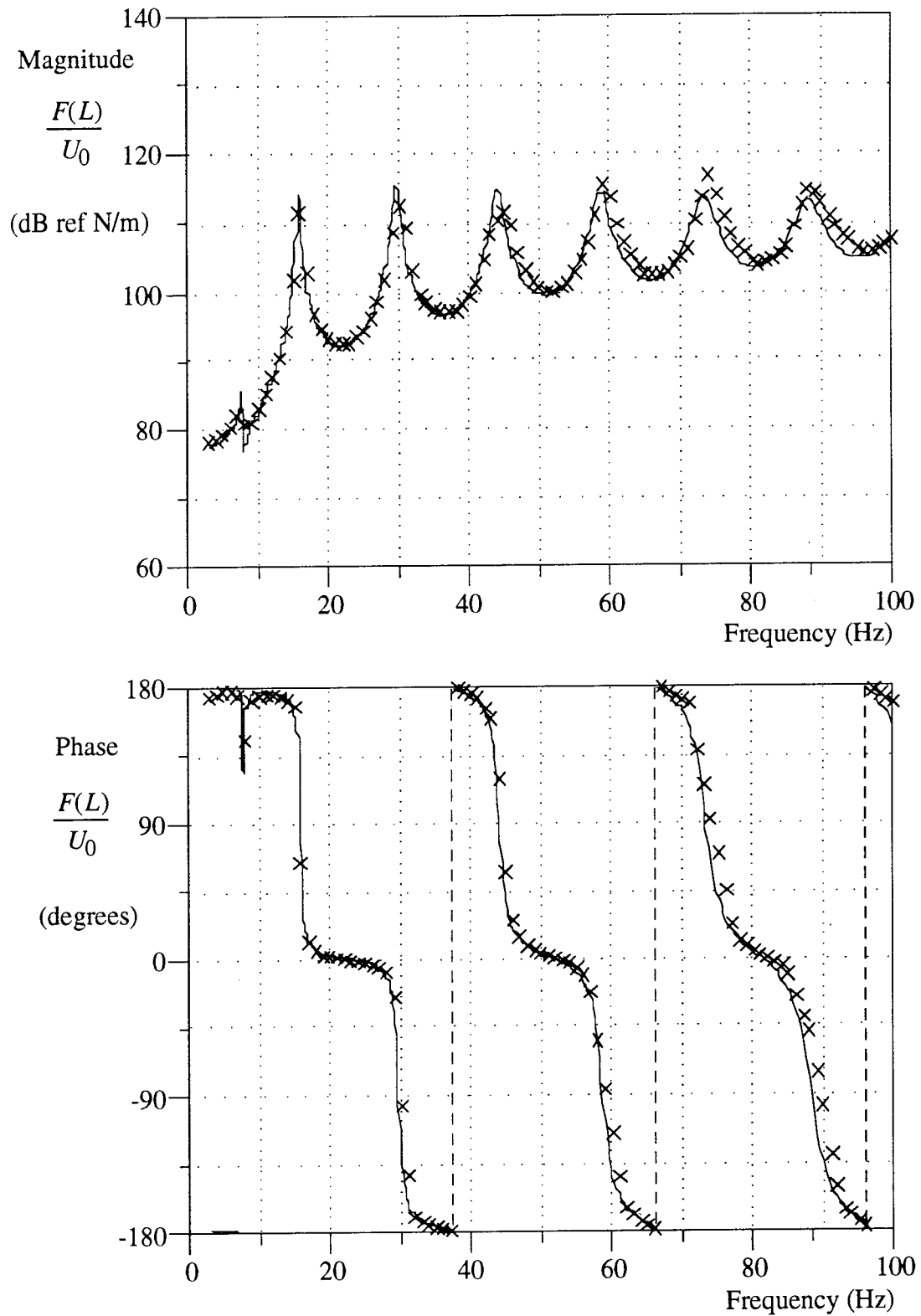With Model Depicted as Solid Line and Experimental Data as X's

Figure 6. Transfer Function of Aft Force Divided by Forward Displacement
With Model Depicted as Solid Line and Experimental Data as X's

## 5. CONCLUSIONS

The axial modulus of a tensioned bar can be calculated from the forward force transducer, forward accelerometer, aft force transducer, and aft accelerometer data. The method yields a value for the modulus at every frequency for which data are collected. The frequency domain values of the modulus can be fit with a curve, and the model can be recalculated with this estimate of the modulus. It was shown that this approach provides a good match between experimental data and the model.

## 6. REFERENCES

1. D. M. Norris, Jr., and W. C. Young, 1970, *Experimental Mechanics*, **10**, 93-96, Complex modulus measurements by longitudinal vibration testing.

2. B. E. Read and G. D. Dean, 1978, *The Determination of Dynamic Properties of Polymers and Composites*, Bristol: Adam Hilger Ltd.

3. W. M. Madigosky and G. F. Lee, 1983, *Journal of the Acoustical Society of America*, **73**(4), 1374-1377, Improved resonance technique for materials characterization.

4. S. L. Garrett, 1990, *Journal of the Acoustical Society of America*, **88**(1), 210-220, Resonant acoustic determination of elastic moduli.

5. H. E. Davis, G. E. Troxell, and C. T. Wiskocil, 1941, *The Testing and Inspection of Engineering Materials*, New York: McGraw-Hill Book Company.

6. C. H. Lin and R. Plunkett, 1989, *Journal of Composite Materials*, **23**, 92-104, A low-frequency axial oscillation technique for composite material damping measurement.

7. Metravib Instruments, 1989, *Metravib Viscoanalyseur User's Guide*, Limonest, France.

8.  T. Pritz, 1982, *Journal of Sound and Vibration*, **81**(3), 359-376, Transfer function method for investigating the complex modulus of acoustic materials:  rod-like specimen.

9.  A. D. Nashif, D. I. G. Jones, and J. P. Henderson, 1985, *Vibration Damping*, New York: John Wiley and Sons.

10. B. J. Dobson, 1987, *Mechanical Systems and Signal Processing*, **1**, 29-40, A straight-line technique for extracting modal properties from frequency response data.

11. B. Lundberg and R. H. Blanc, 1988, *Journal of Sound and Vibration*, **126**(1), Determination of mechanical material properties from the two-point response of an impacted linearly viscoelastic rod specimen.

12. C. Minas and D. J. Inman, 1990, *Journal of Vibration and Acoustics*, **112**(1), Matching finite element models to modal data.

13. H. G. Lee and B. J. Bobson, 1991, *Journal of Sound and Vibration*, **145**(1), 61-81, The direct measurement of structural mass, stiffness and damping properties.

14. S.  Ödeen and B. Lundberg, 1993, *Journal of Sound and Vibration*, **165**(1), 1-8, Determination of complex modulus from measured end-point accelerations of an impacted rod specimen.

15. A. J. Hull, 1994, *Journal of Sound and Vibration*, **177**(5), 611-621, A non-conforming approximate solution to a specially orthotropic axisymmetric thin shell subjected to a harmonic displacement boundary condition.

# INITIAL DISTRIBUTION LIST

| Addressee | No. of Copies |
|---|---|
| Defense Technical Information Center | 12 |
| Naval Sea Systems Command (Capt. G. Kent (PMS-425); M. Basilica (Code 4251); D. Lechner (PMS-42511)) | 3 |
| Office of Naval Research 321 (T. G. Goldsberry, K. Dial) | 2 |
| Program Executive Office, USW/ASTO (Cdr. J. Polcari, W. Chen, A. Hommel, J. Jones, Lcdr. M. Traweek, R. Melusky) | 6 |
| Space and Naval Warfare Systems Command (J. P. Feuillet (PMW-182)) | 1 |
| Michigan State University (C. R. MacCluer, C. J. Radcliffe) | 2 |
| Cambridge Acoustical Associates, Inc. (J. E. Cole, J. M. Garrelick) | 2 |
| Technology Service Corporation (L. W. Brooks) | 2 |